

AD-A150 197

MAGNETIC FIELD INTERACTIONS WITH MATERIAL
DISCONTINUITIES(U) COLORADO STATE UNIV FORT COLLINS
DDPT OF ELECTRICAL ENGINEERING W LORD OCT 84
ARO-17923.1-MS DAAG29-81-K-0115 F/G 20/

1/1

UNCLASSIFIED

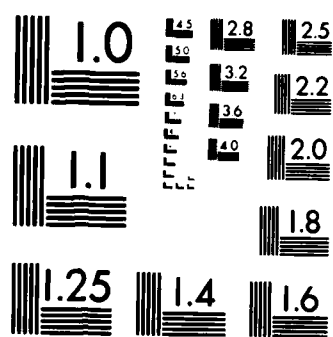
F/G 20/3

HN

END

1. 2. 3. 4. 5. 6. 7. 8. 9. 10. 11. 12. 13. 14. 15. 16. 17. 18. 19. 20. 21. 22. 23. 24. 25. 26. 27. 28. 29. 30. 31. 32. 33. 34. 35. 36. 37. 38. 39. 40. 41. 42. 43. 44. 45. 46. 47. 48. 49. 50. 51. 52. 53. 54. 55. 56. 57. 58. 59. 60. 61. 62. 63. 64. 65. 66. 67. 68. 69. 70. 71. 72. 73. 74. 75. 76. 77. 78. 79. 80. 81. 82. 83. 84. 85. 86. 87. 88. 89. 90. 91. 92. 93. 94. 95. 96. 97. 98. 99. 100. 101. 102. 103. 104. 105. 106. 107. 108. 109. 110. 111. 112. 113. 114. 115. 116. 117. 118. 119. 120. 121. 122. 123. 124. 125. 126. 127. 128. 129. 130. 131. 132. 133. 134. 135. 136. 137. 138. 139. 140. 141. 142. 143. 144. 145. 146. 147. 148. 149. 150. 151. 152. 153. 154. 155. 156. 157. 158. 159. 160. 161. 162. 163. 164. 165. 166. 167. 168. 169. 170. 171. 172. 173. 174. 175. 176. 177. 178. 179. 180. 181. 182. 183. 184. 185. 186. 187. 188. 189. 190. 191. 192. 193. 194. 195. 196. 197. 198. 199. 200. 201. 202. 203. 204. 205. 206. 207. 208. 209. 210. 211. 212. 213. 214. 215. 216. 217. 218. 219. 220. 221. 222. 223. 224. 225. 226. 227. 228. 229. 230. 231. 232. 233. 234. 235. 236. 237. 238. 239. 240. 241. 242. 243. 244. 245. 246. 247. 248. 249. 250. 251. 252. 253. 254. 255. 256. 257. 258. 259. 260. 261. 262. 263. 264. 265. 266. 267. 268. 269. 270. 271. 272. 273. 274. 275. 276. 277. 278. 279. 280. 281. 282. 283. 284. 285. 286. 287. 288. 289. 290. 291. 292. 293. 294. 295. 296. 297. 298. 299. 300. 301. 302. 303. 304. 305. 306. 307. 308. 309. 310. 311. 312. 313. 314. 315. 316. 317. 318. 319. 320. 321. 322. 323. 324. 325. 326. 327. 328. 329. 330. 331. 332. 333. 334. 335. 336. 337. 338. 339. 340. 341. 342. 343. 344. 345. 346. 347. 348. 349. 350. 351. 352. 353. 354. 355. 356. 357. 358. 359. 360. 361. 362. 363. 364. 365. 366. 367. 368. 369. 370. 371. 372. 373. 374. 375. 376. 377. 378. 379. 380. 381. 382. 383. 384. 385. 386. 387. 388. 389. 390. 391. 392. 393. 394. 395. 396. 397. 398. 399. 400. 401. 402. 403. 404. 405. 406. 407. 408. 409. 410. 411. 412. 413. 414. 415. 416. 417. 418. 419. 420. 421. 422. 423. 424. 425. 426. 427. 428. 429. 430. 431. 432. 433. 434. 435. 436. 437. 438. 439. 440. 441. 442. 443. 444. 445. 446. 447. 448. 449. 450. 451. 452. 453. 454. 455. 456. 457. 458. 459. 460. 461. 462. 463. 464. 465. 466. 467. 468. 469. 470. 471. 472. 473. 474. 475. 476. 477. 478. 479. 480. 481. 482. 483. 484. 485. 486. 487. 488. 489. 490. 491. 492. 493. 494. 495. 496. 497. 498. 499. 500. 501. 502. 503. 504. 505. 506. 507. 508. 509. 510. 511. 512. 513. 514. 515. 516. 517. 518. 519. 520. 521. 522. 523. 524. 525. 526. 527. 528. 529. 530. 531. 532. 533. 534. 535. 536. 537. 538. 539. 540. 541. 542. 543. 544. 545. 546. 547. 548. 549. 550. 551. 552. 553. 554. 555. 556. 557. 558. 559. 560. 561. 562. 563. 564. 565. 566. 567. 568. 569. 570. 571. 572. 573. 574. 575. 576. 577. 578. 579. 580. 581. 582. 583. 584. 585. 586. 587. 588. 589. 590. 591. 592. 593. 594. 595. 596. 597. 598. 599. 600. 601. 602. 603. 604. 605. 606. 607. 608. 609. 610. 611. 612. 613. 614. 615. 616. 617. 618. 619. 620. 621. 622. 623. 624. 625. 626. 627. 628. 629. 630. 631. 632. 633. 634. 635. 636. 637. 638. 639. 640. 641. 642. 643. 644. 645. 646. 647. 648. 649. 650. 651. 652. 653. 654. 655. 656. 657. 658. 659. 660. 661. 662. 663. 664. 665. 666. 667. 668. 669. 670. 671. 672. 673. 674. 675. 676. 677. 678. 679. 680. 681. 682. 683. 684. 685. 686. 687. 688. 689. 690. 691. 692. 693. 694. 695. 696. 697. 698. 699. 700. 701. 702. 703. 704. 705. 706. 707. 708. 709. 710. 711. 712. 713. 714. 715. 716. 717. 718. 719. 720. 721. 722. 723. 724. 725. 726. 727. 728. 729. 730. 731. 732. 733. 734. 735. 736. 737. 738. 739. 740. 741. 742. 743. 744. 745. 746. 747. 748. 749. 750. 751. 752. 753. 754. 755. 756. 757. 758. 759. 760. 761. 762. 763. 764. 765. 766. 767. 768. 769. 770. 771. 772. 773. 774. 775. 776. 777. 778. 779. 780. 781. 782. 783. 784. 785. 786. 787. 788. 789. 790. 791. 792. 793. 794. 795. 796. 797. 798. 799. 800. 801. 802. 803. 804. 805. 806. 807. 808. 809. 810. 811. 812. 813. 814. 815. 816. 817. 818. 819. 820. 821. 822. 823. 824. 825. 826. 827. 828. 829. 830. 831. 832. 833. 834. 835. 836. 837. 838. 839. 840. 84

QTHC



MICROCOPY RESOLUTION TEST CHART
NATIONAL BUREAU OF STANDARDS-1963-A

AD-A150 197

engineering

ARO 17923.1-MIS

(2)

Magnetic Field Interactions
with Material Discontinuities

ARO Final Report

October 1984

ONE FILE COPY

Prepared for the U.S. Army Research Office

under Contract DAAG29-81-K-0115

W. Lord, Principal Investigator

85 01 29 100

UNCLASSIFIED

SECURITY CLASSIFICATION OF THIS PAGE (When Data Entered)

| REPORT DOCUMENTATION PAGE | | READ INSTRUCTIONS
BEFORE COMPLETING FORM |
|--|---|---|
| 1. REPORT NUMBER
ARO 17923.1-MS | 2. GOVT ACCESSION NO.
AD A/50 147
N/A | 3. RECIPIENT'S CATALOG NUMBER
N/A |
| 4. TITLE (and Subtitle)
MAGNETIC FIELD INTERACTIONS WITH MATERIAL
DISCONTINUITIES | | 5. TYPE OF REPORT & PERIOD COVERED
15 Jun 81 - 14 Sep 84
Final Report |
| | | 6. PERFORMING ORG. REPORT NUMBER
N/A |
| 7. AUTHOR(s)
W. Lord | | 8. CONTRACT OR GRANT NUMBER(s)
DAAG29-81-K- 0115 |
| 9. PERFORMING ORGANIZATION NAME AND ADDRESS
Department of Electrical Engineering
Colorado State University
Fort Collins, CO 80523 | | 10. PROGRAM ELEMENT, PROJECT, TASK
AREA & WORK UNIT NUMBERS
N/A |
| 11. CONTROLLING OFFICE NAME AND ADDRESS
U. S. Army Research Office
Post Office Box 12211
Research Triangle Park, NC 27709 | | 12. REPORT DATE
October, 1984 |
| 14. MONITORING AGENCY NAME & ADDRESS (if different from Controlling Office)
N/A | | 13. NUMBER OF PAGES |
| | | 15. SECURITY CLASS. (of this report)
Unclassified |
| 16. DISTRIBUTION STATEMENT (of this Report)
Approved for public release; distribution unlimited. | | |
| 17. DISTRIBUTION STATEMENT (of the abstract entered in Block 20, if different from Report)
NA | | |
| 18. SUPPLEMENTARY NOTES
The view, opinions, and/or findings contained in this report are those of the author(s) and should not be construed as an official Department of the Army position, policy, or decision, unless so designated by other documentation. | | |
| 19. KEY WORDS (Continue on reverse side if necessary and identify by block number)
Nondestructive testing, active leakage fields, residual leakage fields, eddy current NDT, numerical modeling, finite element analysis, defect characterization. | | |
| 20. ABSTRACT (Continue on reverse side if necessary and identify by block number)
All methods of nondestructive testing (NDT) rely for their operation on the interaction of an energy source with defects in the material under test. Such interactions are extremely difficult to model analytically because of the awkward boundaries associated with realistic defect shapes and the inherent nonlinear behavior of many material properties. The major contribution of this project work has been to show that finite element analysis techniques can be used to model electromagnetic energy/defect interactions associated | | |

SECURITY CLASSIFICATION OF THIS PAGE(When Data Entered)

Developed code has been used to study probe design, to simulate testing geometries too difficult to replicate in a laboratory environment and to aid in the development of defect characterization algorithms. Original

| | |
|--------------------|-------------------------------------|
| Accession For | |
| NTIS GRA&I | <input checked="" type="checkbox"/> |
| DTIC TAB | <input type="checkbox"/> |
| Unannounced | <input type="checkbox"/> |
| Justification | |
| | |
| By | |
| Date | |
| Distribution Codes | |
| Avail and/or | |
| Restrictions | |

A-1



SECURITY CLASSIFICATION OF THIS PAGE(When Data Entered)

Table of Contents

| | <u>Page No.</u> |
|---------------------------------------|-----------------|
| 1. Background | 3 |
| 2. Summary of Results | 5 |
| 3. Publications | 6 |
| 4. Participating Scientific Personnel | 8 |
| 5. Future Work | 8 |
| 6. References | 9 |
| 7. Appendix I | 12 |
| 7a. Appendix II | 23 |

Magnetic Field Interactions
with Material Discontinuities

by
W. Lord

Abstract

All methods of nondestructive testing (NDT) rely for their operation on the interaction of an energy source with defects in the material under test. Such interactions are extremely difficult to model analytically because of the awkward boundaries associated with realistic defect shapes and the inherent nonlinear behavior of many material properties. The major contribution of this project work has been to show that finite element analysis techniques can be used to model electromagnetic energy/defect interactions associated with active leakage field, residual leakage field, eddy current and pulsed eddy current NDT methods.

Developed code has been used to study probe design, to simulate testing geometries too difficult to replicate in a laboratory environment and to aid in the development of defect characterization algorithms.

1. Background

Electromagnetic methods of nondestructive testing are used widely throughout the aerospace, transportation, ordnance, metals and energy industries for detecting defects in critical metal parts. A major stumbling block in the development of these techniques, particularly with regard to the study of automated defect characterization schemes and associated imaging systems, has been the lack of a suitable model capable of predicting the inherently complex field/defect interactions.

Over the past decade, with Army Research Office support, the NDT laboratory at Colorado State University has pioneered in the use of finite element analysis techniques to solve the modeling problem for active and residual leakage field as well as eddy current NDT methods¹.

With the advent of the digital computer, increasing emphasis has been placed on the numerical solution of partial differential equations. In the late 1960's Erdelyi² showed how the finite difference method of approximating partial derivatives could be applied to the prediction of electromagnetic fields in electrical machinery. At about the same time Winslow³ and Silvester and Chari⁴ demonstrated that finite element techniques, based on variational calculus, could be applied to the same problems. A period of acrimonious debate followed in the power apparatus and systems literature as to the relative merits of the two approaches⁵.

Based on the author's experience in the early 1970's of applying finite element analysis to the study of electromagnetic fields in magnetic structures^{6,7}, it became clear that such techniques would be ideally suited to the study of electromagnetic NDT phenomena because of the ease with which the awkward defect boundaries could be handled.

With a small "seed-money" grant from the Colorado Energy Research

Institute in 1974, initial work was undertaken to develop finite element code for the study of leakage fields around defects in a cylindrical shaped bar carrying an axial dc excitation current - the "active" case. Based on promising preliminary results from the CERI study⁸, a proposal was submitted to the Army Research Office in 1975. The major objectives of the ARO study were to a) extend the preliminary results to a wider variety of defect shapes, b) determine the feasibility of extending the finite element code to the residual leakage field (magnetic particle) NDT situation and c) explore the possibility of applying finite element analysis techniques to a study of eddy current NDT phenomena. Following successful completion of these objectives⁹⁻¹⁴, further work was initiated via an ARO follow-on proposal aimed at extending the studies to:

- a) The examination of an unusual leakage field reversal phenomena¹⁵,
- b) three dimensional magnetostatic finite element code¹⁶,
- c) pulsed eddy current phenomena^{17,18}, and
- d) deconvolution effects in¹⁹ Hall element measurements of magnetostatic leakage fields¹⁹.

In short, Army Research Office support of studies in the Applied Magnetics and NDT Laboratory at Colorado State University relating to electromagnetic field/defect interactions have clearly shown the feasibility and usefulness of applying finite element analysis techniques as a modeling tool^{20,21}. In addition, funding from the Electric Power Research Institute has demonstrated the applicability of such a modeling tool to practical NDT problems of interest to the nuclear industry²²⁻³⁰.

All this work has clearly shown the close interrelationship between models of active, residual and eddy current NDT phenomena, thus paving the way for a unified approach to the problem of modeling electromagnetic field/defect interactions²¹.

In carrying out the modeling studies it has also become apparent that the finite element code has a number of potential uses:

- a) An an "experimental model" for simulation of electromagnetic NDT situations too difficult or expensive to replicate in a laboratory environment.
- b) As an aid to the physical understanding of the interactions between electromagnetic fields and defects in the part under test.
- c) As a design tool for the study of alternative probe geometries.
- d) As a training mechanism for the development of automated defect characterization schemes.
- e) As a technique for estimating the bulk properties (conductivity and permeability) of materials under test. The procedure consists of iterating the finite element code with different property values until the code predictions agree with experimental observations.

2. Summary of Results

Finite element code has been developed for the following electromagnetic NDT testing situations:

- a) Active leakage fields:
 - 1. 2-dimensional.
 - 2. Axisymmetric.
 - 3. 3-dimensional.
- b) Residual leakage fields:
 - 1. 2-dimensional.
- c) Single frequency eddy current:
 - 1. 2-dimensional.
 - 2. Axisymmetric.
 - 3. 3-dimensional.
- d) Pulsed eddy current:
 - 1. Axisymmetric.

In addition, experimental work has been carried out using the test rig

shown schematically in Figure 1. This has allowed confirmation of the developed finite element code and led to some novel studies of leakage field reversal phenomena¹⁵, Hall-element deconvolution¹⁹ and the imaging of magnetostatic leakage fields and eddy current signals³¹ (see Figs. 2 and 3). Initial work has also begun on the application of finite element code to the simulation of ultrasonic NDT phenomena³².

3. Publications

From April 1980 to September 1984 the following journal publications have been written with support from ARO:

A survey of electromagnetic methods of nondestructive testing, Chapter 3 in the text Mechanics of Nondestructive Testing, edited by W. W. Stinchcomb, Plenum Press, 1980, pp. 77-100.

Finite element analysis of eddy current phenomena, Materials Evaluation, Vol. 38, No. 10, Oct. 1980, pp. 39-43.

Development of theoretical models for NDT eddy current phenomena, in Eddy Current Characterization of Materials and Structures, ASTM STP 722, G. B. Birnbaum and G. Free, Eds., ASTM, 1981, pp. 5-21.

Developments in the finite element modeling of eddy current NDT Phenomena at CSU, *ibid*, pp. 357-361.

Numerical modeling of electromagnetic NDT phenomena, in New Procedures in Nondestructive Testing, P. Holler, Editor, Springer-Verlag, 1983, pp. 461-470.

3-D finite element prediction of magnetostatic leakage fields, IEEE Transactions on Magnetism, Vol. MAG-19, No. 5, September 1983, pp. 2260-2265.

Eddy current probe design using finite element analysis, Materials Evaluation, Vol. 41, No. 12, November 1983, pp. 1389-1394 (with N. Ida and R. Palanisamy). ASNT 1984 Achievement Award.

Applications of numerical field modeling to electromagnetic methods of nondestructive testing, IEEE Transactions on Magnetism, Vol. MAG-19, No. 6, November 1983, pp. 2437-2442.

Solution of linear equations for small computer systems, International Journal for Numerical Methods in Engineering, Vol. 20, No. 4, April 1984, pp. 625-641 (with N. Ida).

Superposition of eddy current probe signals, Materials Evaluation, Vol. 42, No. 7, June 1984, pp. 930-933 (with D. Horne and S. Udpa).

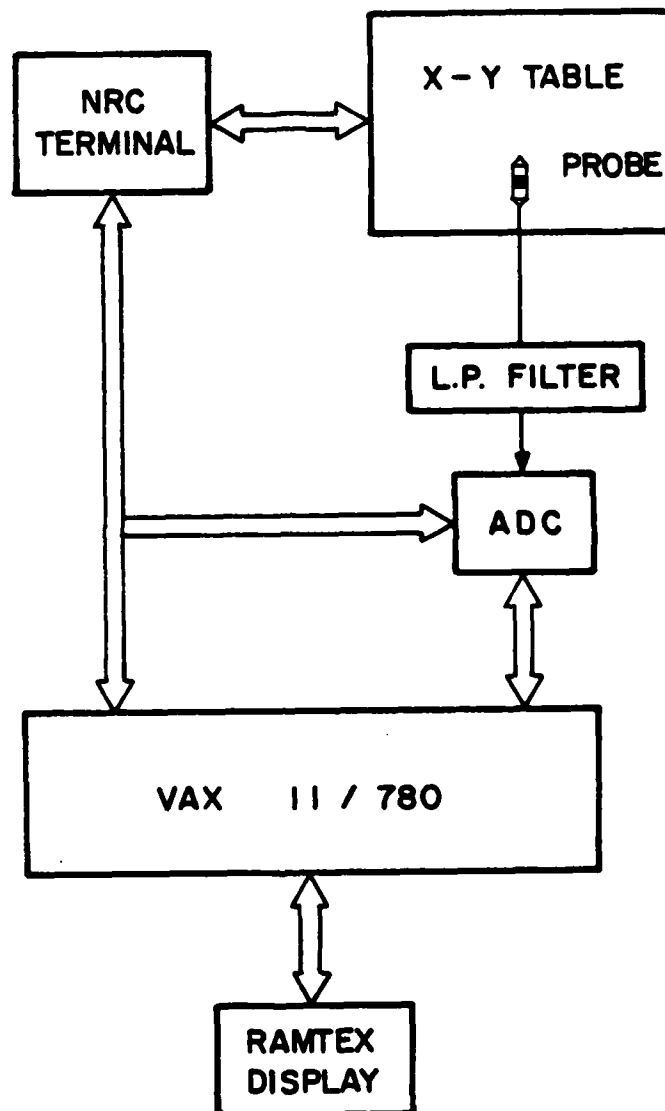


Figure 1. Proposed Imaging System Design.

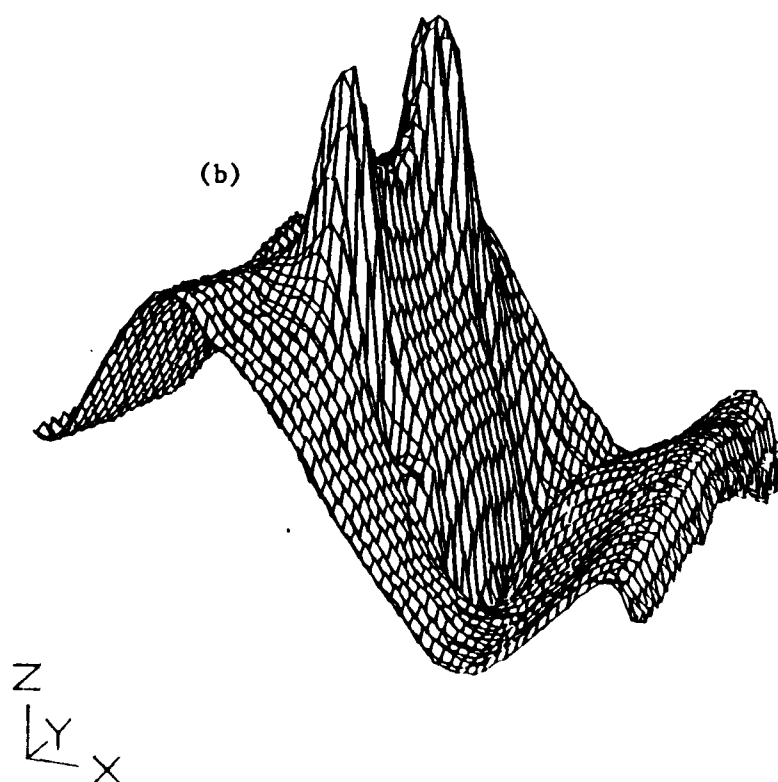
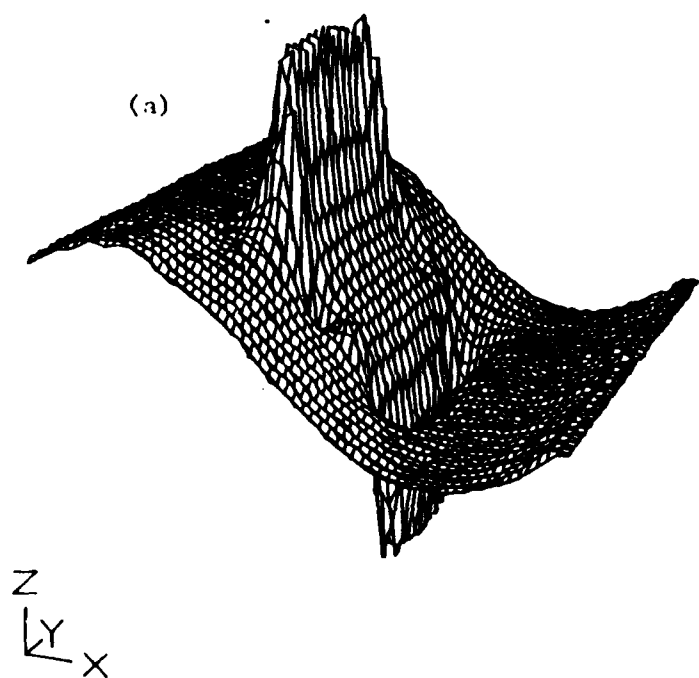


Figure 2. Active (a) and residual (b) leakage field profiles above a rectangular slot in a ferromagnetic bar.

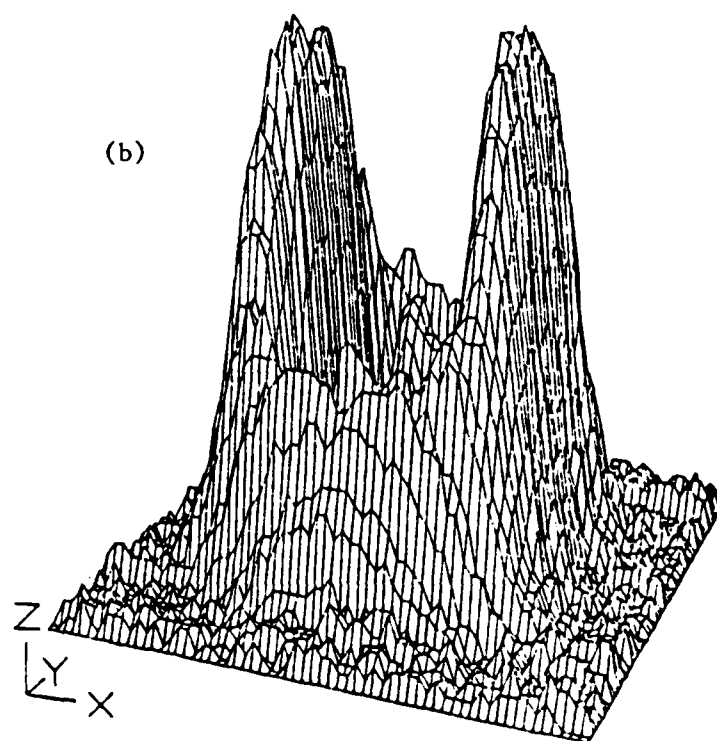
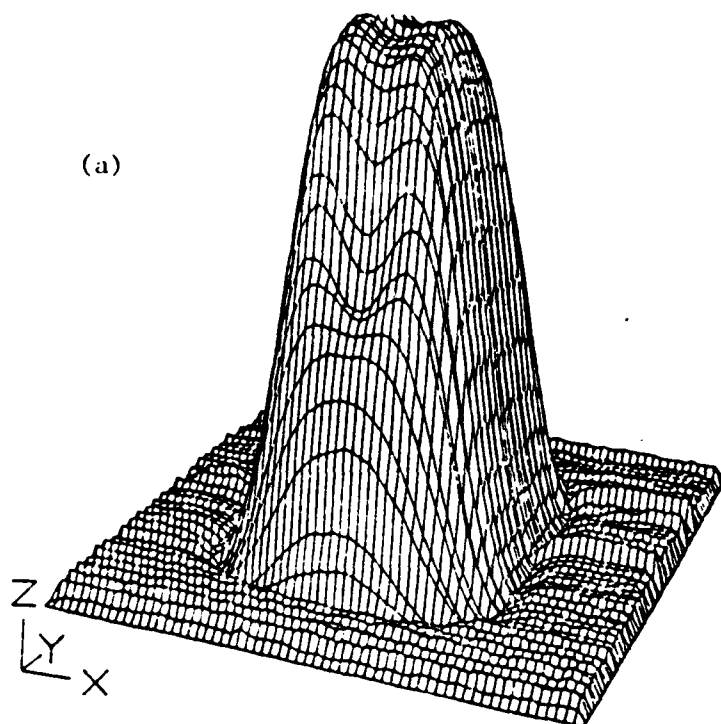


Figure 3. Real (a) and imaginary (b) channel signals from an eddy current probe scanned over a rectangular slot in a ferromagnetic bar.

Finite element modeling of pulsed eddy current phenomena, in Review of Progress in Quantitative Nondestructive Evaluation, D. O. Thompson and D. E. Chimenti, Eds., Plenum, 1984, pp. 561-568 (with B. Allen).

Deconvolution of defect leakage field profiles obtained by using Hall element probes, ibid, pp. 855-862 (with L. Srinivasan).

In addition, the following conference presentations have been made:

Modeling residual and active leakage fields, an invited paper presented at the ASNT Fall Conference, Houston, Oct., 1980.

Recent developments in electromagnetic NDT methods, an invited paper presented at the Symposium on Novel NDE Methods for Materials, AIME Annual Meeting, Dallas, Texas, February 1982.

NDE Education/Training for Engineers, ASME-PVP Annual Meeting, Orlando, June 1982.

Numerical modeling of electromagnetic NDT phenomena, an invited paper presented at the German-American Workshop on NDT Research and Development, Saarbrücken, W. Germany, August 1982.

Eddy current techniques and their potential for determining material properties, an invited paper presented at the Symposium on Nondestructive Methods for Material Property Determination, Hershey, PA, April 1983.

Applications of numerical field modeling to electromagnetic methods of NDT, an invited paper presented at COMPUMAG, Genoa, Italy, May 1983.

Residual and active magnetic leakage field modeling, presented at QualTest II, Dallas, October 1983.

Numerical modeling of eddy current NDE, an invited paper presented at the 29th Annual Conference on Magnetism and Magnetic Materials, Pittsburgh, November 1983.

The case for numerically modeling electromagnetic NDT phenomena, presented at the Seminar on Nondestructive Inspection of Ferromagnetic Materials, Dresser Industries, Houston, March, 1984.

A new technique for modeling hysteresis loop phenomena, presented at an Eddy Current Seminar, Rutherford Appleton Laboratory, Abingdon, Oxford, U.K., April 1984.

NDT Education at Colorado State University, The case for numerical modeling of electromagnetic NDT phenomena, both papers presented at the ASNT Spring Conference, Denver, May 1984.

Nondestructive evaluation in electrical engineering, presented at the ASEE Annual Conference, Salt Lake City, June 1984.

Diffusion, waves, phase and eddy current imaging, presented at the Review of Progress in Quantitative NDE, La Jolla, CA, July 1984 (with L. Udpa).

A finite element formulation for ultrasonic NDT modeling, presented at the Review of Progress in Quantitative NDE, La Jolla, CA, July 1984 (with R. Ludwig).

4. Participating Scientific Personnel

Several graduate students have been associated with the project during the 1980-84 time frame including:

- R. Palanisamy - Ph.D., 1980. Currently a senior NDT research engineer with the Timken Co., Canton, Ohio.
- S. Udpa (Satish) - Ph.D., 1983. Currently an Assistant Professor of Electrical Engineering, Colorado State University.
- N. Ida - Ph.D., 1983. Currently an Assistant Professor of Electrical Engineering, University of Akron.
- L. Udpa (Srinivasan) - Ph.D. student at Colorado State University.
- R. Ludwig - Ph.D. student at Colorado State University.
- B. L. Allen - M.S., 1983. Research engineer with Rockwell International.
- S. Heath - M.S., 1983, Engineer with Hewlett Packard.
- C. Wang - Currently completing his Ph.D. degree at North Carolina.

W. Lord has been principal investigator throughout.

5. Future Work

This project has clearly shown the feasibility of applying finite element analysis to the modeling of all electromagnetic NDT phenomena. Additional funding has been requested from ARO to extend this work to the application of imaging for the display of results from electromagnetic NDT methods. Use of the finite element code will aid in the development of imaging inverse algorithms.

6. References

1. Lord, W.: Magnetic field interactions with material discontinuities. ARO Final Progress Report, DAAG29-76-G-0249, April, 1980.
2. Erdelyi, E. A.: et al. Nonlinear magnetic field analysis of dc machines. IEEE Trans. PAS. 89 (1970) 1546-1583.
3. Winslow, A. M.: Numerical solution of the quasilinear Poisson equation in a nonuniform triangle mesh. J. Comp. Phys. 2 (1967) 149-172.
4. Silvester, P., Chari, M.V.K.: Finite element solution of saturable magnetic field problems. IEEE Trans. PAS. 89 (1970) 1642-1651.
5. Demerdash, N. A., Nehl, T. W.: An evaluation of the methods of finite elements and finite differences in the solution of nonlinear electromagnetic fields in electrical machines. IEEE Trans. PAS. 98 (1979) 74-87.
6. Lord, W., Hwang, J. H.: Convergence and mesh subdivision for finite element analysis of nonlinear magnetic fields. Int. J. Comp. Elec. Eng. 1 (1974) 513-520.
7. Hwang, J. H., Lord, W.: Finite element analysis of the magnetic field distributions inside a rotating ferromagnetic bar. IEEE Trans. MAG. 10 (1974) 513-520.
8. Lord, W., Hwang, J. H.: Finite element modeling of magnetic field defect interactions. ASTM. J. Test, Eval. 3 (1975) 21-25.
9. Lord, W., Hwang, J. H.: Defect characterization from magnetic leakage fields. Brt. J. NDT. 19 (1977) 14-18.
10. Lord, W.: et al. Residual and active leakage fields around defects in ferromagnetic materials. Mat. Eval. 36 (1978) 47-54.
11. Palanisamy, R., Lord, W.: Finite element modeling of electromagnetic NDT phenomena, IEEE Trans. MAG, 15 (1979) 1479-1481.
12. Lord, W.: A survey of electromagnetic methods of nondestructive testing. Mechanics of Nondestructive Testing, Stinchcomb, W. W. (ed.) Plenum Press (1980) 77-100.
13. Palanisamy, R., Lord, W.: Finite element analysis of eddy current phenomena, Mat. Eval. 18 (1980) 39-41.
14. Lord, W., Palanisamy, R.: Development of theoretical models for NDT eddy current phenomena, in Eddy Current Characterization of Materials and Structures, ASTM STP 722, Birnbaum, G. B. and Free, G., Eds., ASTM (1981) 5-21.

15. Heath, S. E.: Residual and active leakage field modeling. M.S. Thesis, Colorado State University, 1984.
16. Ida, N., Lord, W.: 3-D finite element prediction of magnetostatic leakage fields, IEEE Trans. 19 (1983) 2260-2265.
17. Allen, B. L.: Finite element modeling of pulsed electromagnetic NDT phenomena. M.S. Thesis, Colorado State University, 1984.
18. Allen, B. L., Lord, W.: Finite element modeling of pulsed eddy current phenomena, in Review of Progress in Quantitative Nondestructive Evaluation, D. O. Thompson and D. E. Chimenti, Eds., Plenum (1984).
19. Srinivasan, L., Lord, W.: Deconvolution of defect leakage field profiles obtained by using Hall element probes, ibid, 855-862.
20. Lord, W.: Numerical modeling of electromagnetic NDT phenomena, in New Procedures in Nondestructive Testing, Holler, P., Ed., Springer-Verlag 81983) 461-470.
21. Lord, W.: Applications of numerical field modeling to electromagnetic methods of nondestructive testing, IEEE Trans. Mag. 19 (1983) 2437-2442.
22. Palanisamy, R., Lord, W.: Detection and modeling magnetite buildup in steam generators, IEEE Trans. Mag. 16 (1980) 695-697.
23. Palanisamy, R., Lord, W.: Prediction of eddy current probe signal trajectories, IEEE Trans. Mag. 16 (1980) 1083-1085.
24. Palanisamy, R., Lord, W.: Magnetic probe inspection of steam generator tubing, Mat. Eval. 38 (1980) 38-40.
25. Lord, W., Palanisamy, R., Satish, S. R.: Electromagnetic methods of detecting magnetite in PWR steam generators, in both Quantitative NDE in the Nuclear Industry, R. B. Clough, Editor, American Society for Metals f81983) 106-109, and Mat. Energy Sys. 5, (1983) 112-116.
26. Ida, N., Lord, W.: Graphical simulation of electromagnetic NDT probe fields, IEEE Com. Graphics Appl. (1983) 21-28.
27. Palanisamy, R., Lord, W.: Sensitivity analysis of a variable reluctance probe for steam generator tubing inspection, IEEE Trans. Mag. 19 (1983) 2219-2221.
28. Palanisamy, R., Lord, W.: Prediction of eddy current signals for nondestructive testing of condenser tubing. ibid, 2213-2215.
29. Ida, N., Betzold, K., Lord, W.: Finite element modeling of absolute eddy current probe signals, NDT (1983) 147-154.
30. Ida, N., Palanisamy, R., Lord, W.: Eddy current probe design using finite element analysis, Mat. Eval. 41 (1983) 1389-1394.

31. Udpa, L., Lord, W.: Diffusion, waves, phase and eddy current imaging, Review of Progress in Quantitative NDE, La Jolla, July, 1984.
32. Ludwig, R., Lord, W.: A finite element formulation for ultrasonic NDT modeling, *ibid.*

7. Appendix I

"Diffusion, Waves, Phase and Eddy Current Imaging."

L. Udpa and W. Lord

A paper presented at the Review
of Progress in Quantitative NDE,
La Jolla, July 1984.

DIFFUSION, WAVES, PHASE AND EDDY

CURRENT IMAGING

L. Udpa and W. Lord

Electrical Engineering Department
Colorado State University
Fort Collins, CO 80523

INTRODUCTION

The discovery of electromagnetic induction by Faraday and Henry in 1831 not only served as the catalyst needed for the very creation of electrical engineering but also provided the physical basis for eddy current nondestructive testing (NDT) as we know it today and as first realized in the classical experiments of Hughes¹. As this fundamental work preceded Maxwell's prediction of electromagnetic wave phenomena by over half a century, it may seem somewhat surprising to the casual reader that there should be any need to explain why eddy current NDT phenomena can be classified as quasi-static in nature with none of the attributes of classical electromagnetic waves. Unfortunately, there are many misconceptions concerning the wave-like nature of eddy current NDT phenomena which have even led to the suggestion² that conventional eddy current NDT probe signals can be treated holographically. There are several reasons for the existence of these misconceptions:

1. Many papers in the field (see for example Hochschild³) describe the propagation of an electromagnetic plane wave in a medium as being analogous to eddy current NDT phenomena. Although the analog itself has some limited validity, it is rarely if ever mentioned that a conventional eddy current NDT probe does not launch an electromagnetic wave (as does say an antenna).

2. Solution of the quasi-static skin effect equation for current density does have the same form as would a damped electromagnetic wave. However, this is more a statement of the consistency of Maxwell's equations across different regimes (see Figure 1) than support for eddy current waves. A number of authors address this seemingly anomalous situation (see for example, Stoll⁴, Ferrari⁵, and Melcher⁶) and clearly differentiate between electromagnetic diffusion and electromagnetic wave phenomena.

3. Much of the terminology associated with eddy current NDT phenomena (phase, for example) has a direct counterpart in electromagnetic wave parlance.

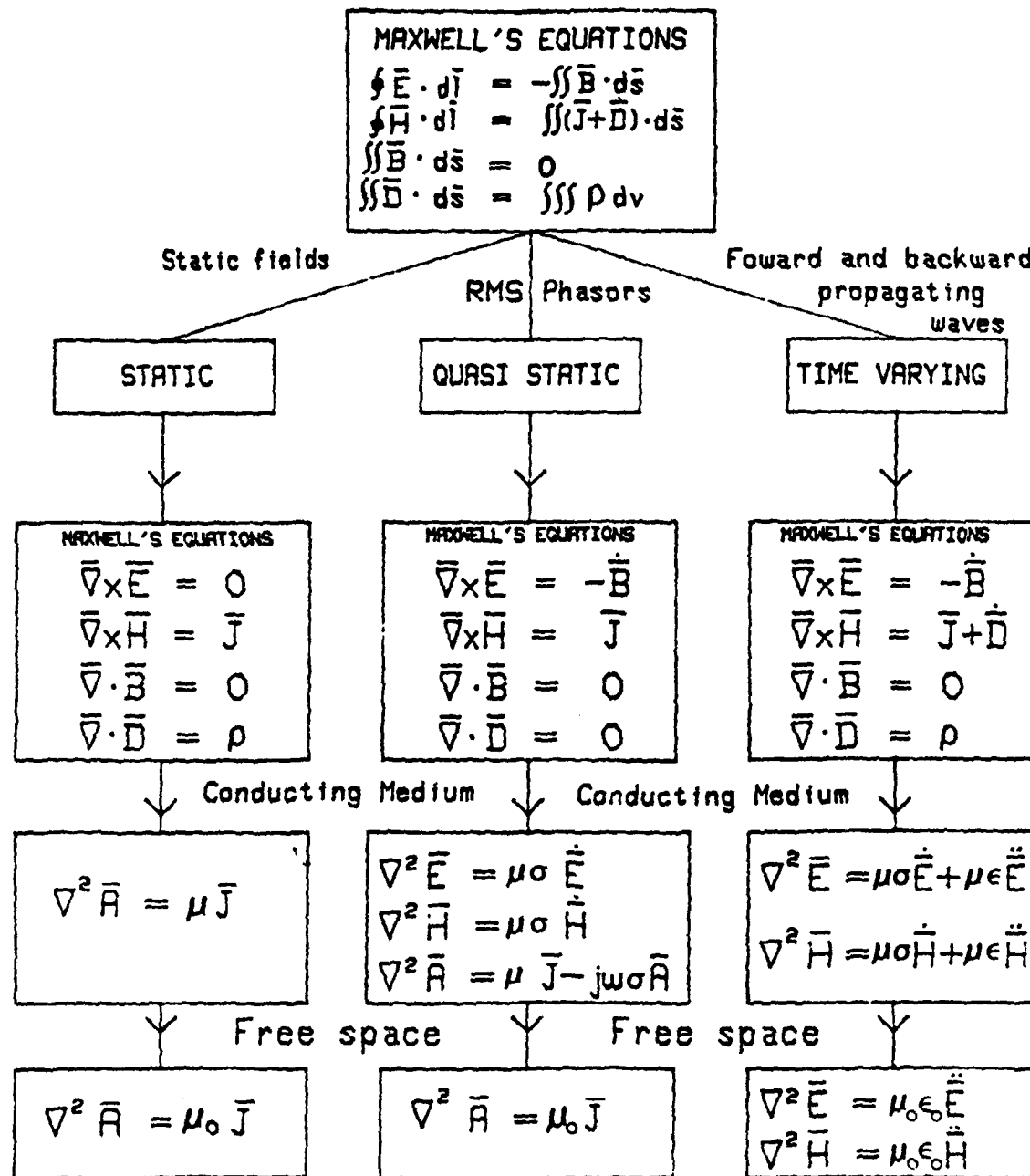


Figure 1. Overview of Maxwell's equation in different frequency regimes.

Conventional eddy current NDT phenomena are truly steady-state alternating-current induction phenomena completely describable by quasi-static field theory. The following sections of this paper expand on these comments and discuss their implications for eddy current imaging.

PRINCIPLES OF EDDY CURRENT TESTING

As stated in the introduction, the eddy current method of nondestructive testing is principally based on Faraday's law of electromagnetic induction. When a coil excited by an alternating current source is brought close to a conducting material, the primary field set up by the coil induces eddy currents in the material, setting up an opposing, secondary field. In a nonmagnetic test object, this results in a reduction of the net flux linkages of the coil, thereby reducing the inductance of the coil. The resistance measured at the terminals of the coil is also altered to account for the eddy current losses within the material. The presence of a defect or inhomogeneity in the material causes a redistribution of the eddy currents, thereby changing the complex impedance of the probe coil. Changes in the coil impedance caused by defects in the material are represented as trajectories in the impedance plane and used for defect characterization.

From considerations of the operating frequencies and dimensions of the experimental set-up, the eddy currents constitute a quasi-static phenomenon. Under these conditions the displacement current is neglected and Maxwell's equations are

$$\nabla \times \bar{E} = - \frac{\partial \bar{B}}{\partial t} \quad (1)$$

$$\nabla \times \bar{H} = \bar{J} \quad (2)$$

$$\nabla \cdot \bar{B} = 0 \quad (3)$$

$$\nabla \cdot \bar{D} = 0 \quad (4)$$

Assuming a linear, isotropic and homogeneous medium the constitutive relations are

$$\bar{B} = \mu \bar{H} \quad (5)$$

$$\bar{D} = \epsilon \bar{E} \quad (6)$$

$$\bar{J} = \sigma \bar{E} \quad (7)$$

Decoupling equations (1) and (2) using the constitutive relations, the governing equations for the fields and currents are

$$\nabla^2 \bar{E} = \mu \sigma \frac{\partial \bar{E}}{\partial t} \quad (8)$$

$$\nabla^2 \bar{H} = \mu \sigma \frac{\partial \bar{H}}{\partial t} \quad (9)$$

$$\nabla^2 \bar{J} = \mu\sigma \frac{\partial \bar{J}}{\partial t} \quad (10)$$

For single frequency sinusoidal excitation, the one-dimensional form of (10) can be written in the phasor form as

$$\frac{d^2 \bar{J}}{dx^2} = j\omega\mu\sigma \bar{J} \quad (11)$$

The steady, state solution for the case of a sheet of alternating current density at the surface of a semi-infinite medium is given by

$$\bar{J}(x,t) = \bar{J}(0,t) \exp\left(-\frac{x}{\delta}\right) \exp\{-j(\frac{x}{\delta} - \omega t)\} \quad (12)$$

where the skin depth δ is given by

$$\delta = \left(\frac{2}{\omega\mu\sigma}\right)^{1/2} \quad (13)$$

Though equation (12) has the mathematical properties of an attenuated wave it does not describe a true physical wave. What it actually describes is the distribution of steady state alternating currents whose magnitude decays exponentially and whose phase angle varies linearly with depth according to the relations

$$J(x) = J(0) e^{-x/\delta} \quad (14)$$

$$\theta(x) = \left(\frac{\omega\mu\sigma}{2}\right)^{1/2} x \quad (15)$$

Equations (12) - (15) are derived for a rather contrived geometry for the sake of computational ease. The eddy current paths in an actual eddy current test are far more complex and the presence of anomalies in the medium further perturb this distribution. However the solutions obtained above do serve to illustrate the general behavior of fields and currents and the associated skin depth which is of significant importance in eddy current NDT situations.

The phase and magnitude described above for a prescribed depth are not experimentally measurable. What is measured in an eddy current test is the complex impedance of the probe coil, which is affected by the total eddy current distribution in the test specimen.

The measured impedance of the coil can be expressed as

$$\bar{z}_c = \frac{\bar{V}}{\bar{I}} = R_c + jX_c = |z_c| \angle \phi_c \quad (16)$$

where \bar{V} and \bar{I} are RMS valued voltage and current phasors.

The phase angle of the eddy current test data is then given by

$$\phi_c = \tan^{-1}\left(\frac{X_c}{R_c}\right) \quad (17)$$

which does not have a simple, direct relationship with the θ of equation (15).

The eddy current test can be compared to the operation of a transformer where the probe coil is the primary and the test material constitutes the secondary. Just as in a transformer, the secondary properties are referred to the primary side and hence the material characteristics are reflected in the coil impedance measurement. However this measurement reveals nothing about the actual current distribution within the test specimen. Determination of material characteristics on the basis of the test signal from the eddy current probe is therefore a complex process.

IMAGING

Imaging or inversion of eddy current data is the problem of reconstruction of the defect in three dimensions, given the measured signal. A direct approach by use of a theoretical model based on the underlying physical process is too complex and most of the existing defect characterization schemes resort to the indirect algorithmic methods which depend on characteristic features in the signal for classification information.

HOLOGRAPHIC IMAGING

In an attempt to directly image the defect in three dimensions, Hildebrand et al.² apply holographic principles to eddy current data, interpreting the eddy current phenomenon as an interference between incident and reflected electromagnetic waves. The magnitude and phase of the coil impedance data in (16) are thus interpreted as the magnitude and phase of a scattered wavefront that satisfies the Helmholtz wave equation. The method then applies a backward wave propagation² algorithm to the eddy current data to reconstruct the defect in three dimensions.

This procedure gives meaningful results only if the data input to it indeed describes a true wave. Otherwise, the method functions as a low pass filter with a phase response given by

$\left[\frac{2\pi}{\lambda} \{1 - (\lambda u)^2 - (\lambda v)^2\}^{1/2} z \right]$ which merely distorts the eddy current probe signals.

ALGORITHMIC IMAGING

Algorithmic imaging is a procedure for deducing defect geometry parameters by using distinctive properties of the measured signal. The algorithmic methods for characterizing and sizing defects include signal processing techniques such as adaptive learning networks⁷, and the use of Fourier descriptors developed by Udpa and Lord⁸. In all these methods, the eddy current probe signals are treated as signatures of the defect that produced them. The signal from each defect type is then represented by a set of features either from the time domain or frequency domain or a combination of both. A data bank of feature vectors corresponding to all the expected defect types is thus built. An unknown signal is then classified as belonging to one of the sets in the data base by pattern recognition techniques.

A more direct approach has been used by Copley⁹ where the phase and amplitude of the measured signal are directly interpreted in terms of defect dimensions by use of a set of calibration curves.

For the sake of comparing the results of holographic imaging and algorithmic imaging a simple image processing algorithm was implemented. Using the experimental set up shown in Figure 2, the horizontal and vertical channels of the complex probe data were sampled at discrete spatial points digitized and stored on the VAX 11/780 computer. The aluminum bar containing defect patterns such as that shown in Figure 3 was used as the test specimen. Scanning was done on the other side of bar, so that these 90% through-wall holes served as subsurface defects. In Figure 4 the complex data is displayed as four different grey-level coded images representing vertical channel data, horizontal channel data, magnitude and phase. The result of holographic imaging is shown in Figure 5 where the probe data is 'back propagated' to the plane of the defect. The result of a basic thresholding and edge detection algorithm is shown in Figure 6. This algorithm also computes the diameters of the holes. Space limitations preclude a complete discussion of all the test results comparing holographic and algorithmic imaging results. The reader is left to draw his own conclusions from Figures 5 and 6.

CONCLUSIONS

Holographic imaging algorithms can certainly be applied to the analysis of conventional eddy current probe data. The key questions highlighted by this paper are:

1. Does such a procedure make any physical sense?
2. Does such a procedure have distinct advantages over algorithmic imaging?

In answer, eddy current phenomena are quasi-static phenomena where the operating frequencies and characteristic dimensions are such that the displacement current is negligible. Consequently the eddy currents are described by diffusing phasors rather than by attenuated waves. Secondly, in an eddy current test the measured probe impedance is caused by the integrated effect of all the currents in the specimen and hence the phase of the test data cannot represent the phase of induced eddy currents or the phase of an electromagnetic wave. Thus the indirect nature of the eddy current test makes a direct approach to the inverse problem very complex and algorithmic methods appear to be a more practical solution.

ACKNOWLEDGMENTS

This work results from studies of electromagnetic NDT phenomena funded by the Army Research Office and the Electric Power Research Institute. Long hours of debate, discussion and diatribe with S. Udpa, N. Ida and V. N. Bringi are greatly appreciated.

REFERENCES

1. D. E. Hughes, Induction-balance and experimental researchers therewith, Phil. Mag. 8:50 (1879).
2. B. P. Hildebrand and G. L. Fitzpatrick, Inversion of eddy current data using holographic principles, Review of Progress in Quantitative NDE, La Jolla, 1984.
3. R. Hochschild, Electromagnetic methods of testing metals, in "Progress in non-destructive testing," Vol. 1, E. G. Stanford et al., Macmillan, New York, 1959.
4. R. L. Stoll, "The Analysis of Eddy Currents," Oxford University Press, 1974.
5. R. L. Ferrari, "An Introduction to Electromagnetic Fields," Van Nostrand Reinhold, New York, 1975.
6. J. R. Melcher and H. H. Woodson, "Electromechanical Dynamics," Part I, Wiley, New York, 1968.
7. A. G. Ivakhnenko, The group method of data handling - a rival of the method of stochastic approximation, Soviet Automatic Control, 13:43 (1968).
8. S. S. Udpa and W. Lord, A Fourier descriptor classification scheme for differential probe signals, Materials Evaluation, 42:1136 (1984).
9. D. C. Copley, Eddy current imaging for defect characterization, in "Review of Progress in Quantitative Nondestructive Evaluation," D. Thompson and D. Chimenti eds., Plenum, New York (1984).

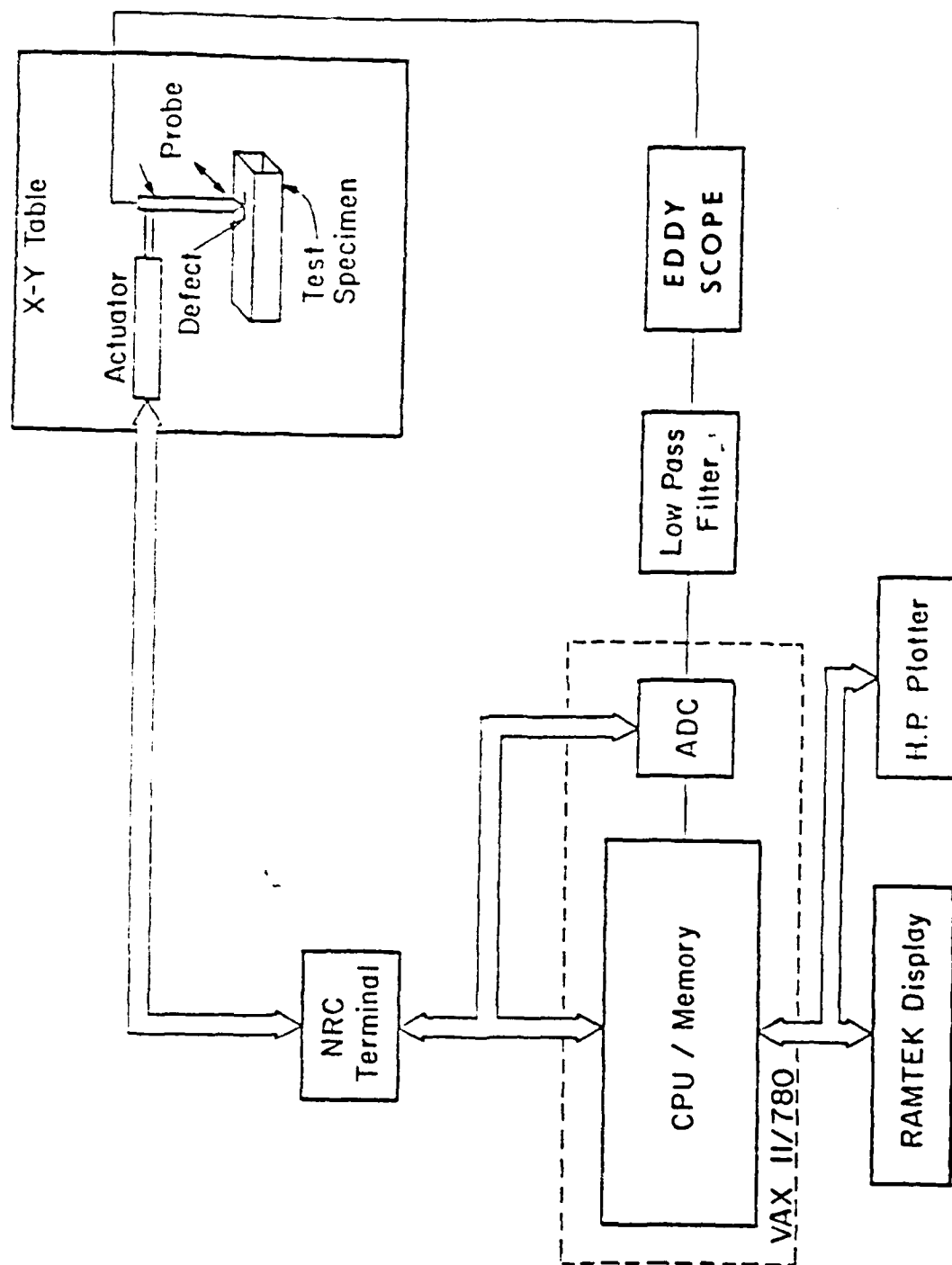


Figure 2. Data acquisition system.



Figure 3. Al bar with defect patterns.

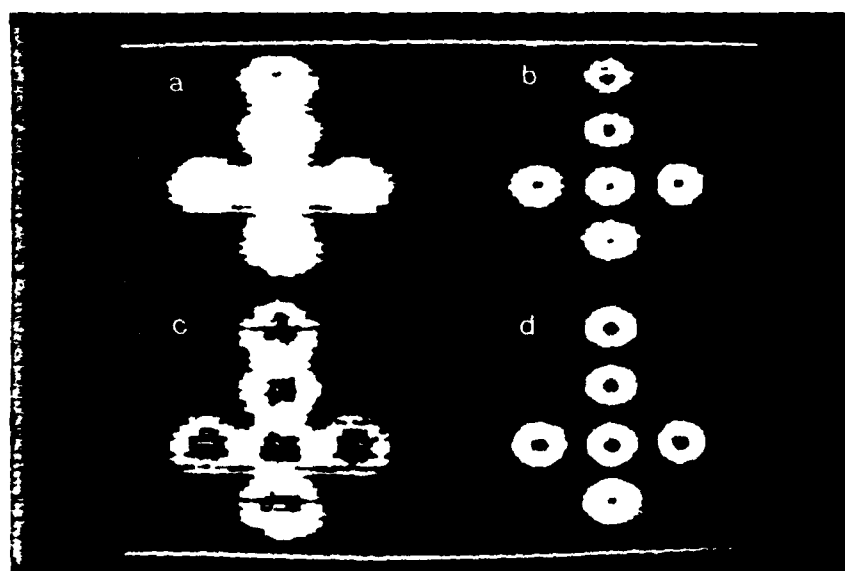


Figure 4. Images of a) horizontal channel, b) vertical channel, c) magnitude, d) phase of eddy current data.

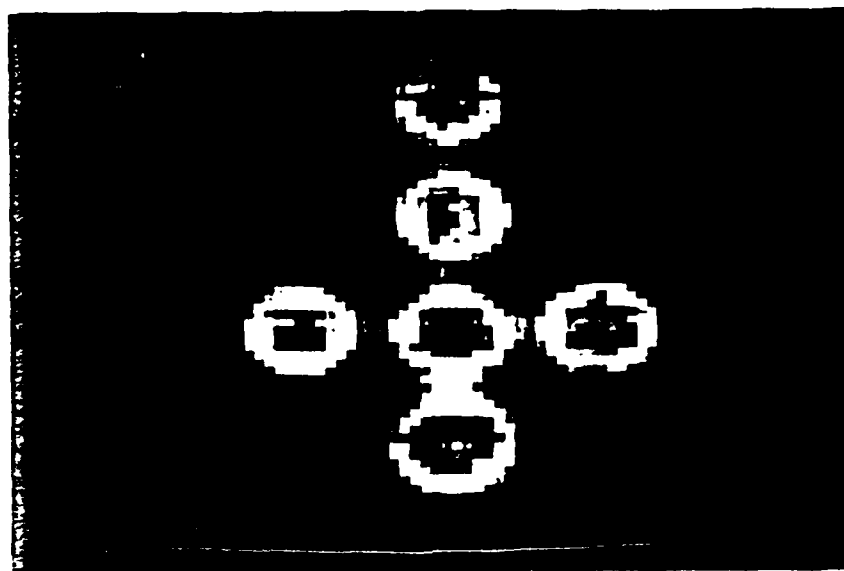


Figure 5. Results of holographic imaging using magnitude and phase data.

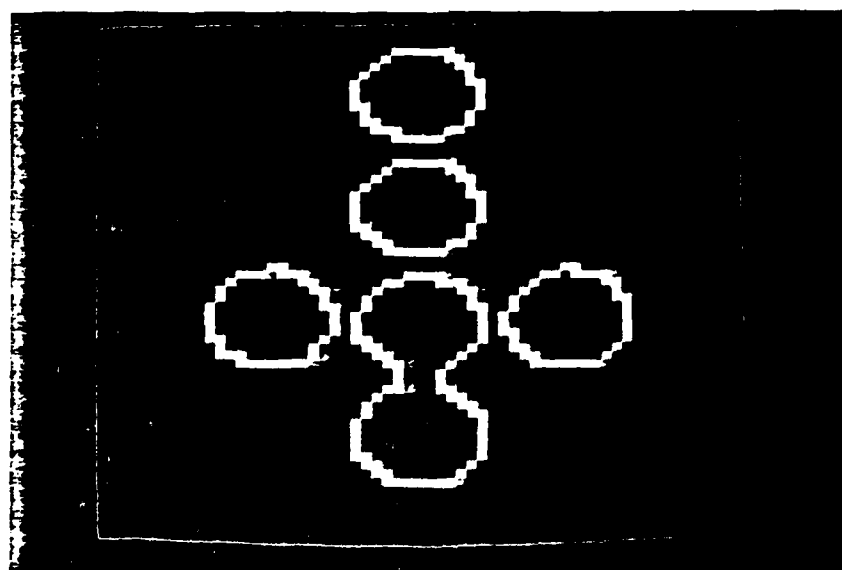


Fig. 6. Results of an edge detection algorithm on Fig. 4d.

7a. Appendix II

"A Finite Element Formulation for Ultrasonic NDT Modeling."

R. Ludwig and W. Lord

A paper presented at the Review
of Progress in Quantitative NDE,
La Jolla, July 1984.

A FINITE ELEMENT FORMULATION FOR

ULTRASONIC NDT MODELING

R. Ludwig and W. Lord

Electrical Engineering Department
Colorado State University
Fort Collins, CO 80523

INTRODUCTION

Numerical analysis techniques have been successfully applied to the modeling of electromagnetic field/defect interactions¹. Studies of magnetostatic leakage field and eddy current NDT phenomena have clearly shown that finite element codes can be used effectively for probe design and the simulation of test geometries difficult to replicate in the laboratory³. In extending these codes to three dimensional geometries and pulsed eddy current phenomena⁵, it was realized that the required computing capability should also be sufficient to model ultrasound/defect interactions directly in the time domain. Increasing availability of powerful vector computers⁶ bodes well for the ultimate solution of the generic NDT problem in which it is desired to predict the probe response to any arbitrarily shaped defect. As a first step in this direction, the NDT research group at Colorado State University, following the pioneering numerical efforts of Bond⁷ and Dewey⁸, has developed a finite element code for direct time domain solution of the elastic wave equation (Figure 1 shows the relationship between numerical and analytical approaches). The following sections describe the finite element formulation and the application of the code to the prediction of 2-D displacements in a rectangular bar excited at one end by a step input of force.

FORMULATION

The general equation of motion can be written in the form

$$\nabla \cdot \underline{\underline{T}} + \underline{\underline{F}} = \rho \frac{\partial^2 \underline{\underline{u}}}{\partial t^2} \quad (1)$$

where $\underline{\underline{T}}, \underline{\underline{F}}, \underline{\underline{u}}$ represent stress tensor, body force and displacement vectors respectively. ρ denotes the material density. Three restrictions are imposed:

- 1) no body forces

$$\underline{\underline{F}} = 0$$

- 2) no internal energy losses and small deformations such that Hook's law is applicable

$$\underline{T} = \underline{C} : \underline{S}$$

with \underline{C} being the fourth rank material tensor and \underline{S} representing the strain tensor

- 3) only a homogeneous isotropic solid is considered. Thus, the material tensor consists of only two independent coefficients λ and μ (Lame constants)

$$C_{ijkl} = \lambda \delta_{ij} \delta_{kl} + \mu (\delta_{ik} \delta_{jl} + \delta_{il} \delta_{jk})$$

Substitution of these three conditions into (1) yields the elastic wave equation in rectangular coordinates

$$(\mu + \lambda) \nabla (\nabla \cdot \bar{u}) + \mu \nabla^2 \bar{u} = \rho \frac{\partial^2 \bar{u}}{\partial t^2} \quad (2)$$

If $V_L^2 = (\lambda + 2\mu)/\rho$ and $V_s^2 = \mu/\rho$ are introduced as longitudinal and shear velocities, (2) can be expressed for the two dimensional case as

$$V_L^2 \frac{\partial^2 u_x}{\partial x^2} + V_s^2 \frac{\partial^2 u_x}{\partial y^2} + (V_L^2 - V_s^2) \frac{\partial^2 u_y}{\partial x \partial y} = \frac{\partial^2 u_x}{\partial t^2} \quad (3a)$$

$$V_L^2 \frac{\partial^2 u_y}{\partial y^2} + V_s^2 \frac{\partial^2 u_y}{\partial x^2} + (V_L^2 - V_s^2) \frac{\partial^2 u_x}{\partial y \partial x} = \frac{\partial^2 u_y}{\partial t^2} \quad (3b)$$

with the Neumann type boundary conditions given by

$$T_{xx}/\rho = V_L^2 \frac{\partial u_x}{\partial x} + (V_L^2 - 2V_s^2) \frac{\partial u_y}{\partial y} \quad (4a)$$

$$T_{xy}/\rho = V_s^2 \left(\frac{\partial u_x}{\partial y} + \frac{\partial u_y}{\partial x} \right) = T_{yx}/\rho \quad (4b)$$

$$T_{yy}/\rho = V_L^2 \frac{\partial u_y}{\partial y} + (V_L^2 - 2V_s^2) \frac{\partial u_x}{\partial x} \quad (4c)$$

FINITE ELEMENT IMPLEMENTATION

Instead of developing a direct discretization of (3) by means of collocation or Galerkin's method, we consider an energy related functional

$$\bar{F}(\bar{u}) = \int \underline{S} : \underline{T} dV + \int \bar{u} \frac{\partial^2 \bar{u}}{\partial t^2} \rho dV$$

or

$$\bar{F}(\bar{u}) = \frac{1}{2} \int (V_L^2 [(\frac{\partial u_x}{\partial x})^2 + (\frac{\partial u_y}{\partial y})^2] + 2(V_L^2 - 2V_s^2) \frac{\partial u_y}{\partial y} + V_s^2 (\frac{\partial u_x}{\partial y} + \frac{\partial u_y}{\partial x})^2 + 2(u_x \frac{\partial^2 u_x}{\partial t^2} + u_y \frac{\partial^2 u_y}{\partial t^2})) \rho dV \quad (5)$$

which, upon finding a stationary value with respect to the unknown displacements u_x, u_y , results in the same solution. An easy way to check the correctness of the above functional is to utilize variational calculus in order to arrive at the so called Euler equations which subsequently yield the original elastic wave equations (3a) and (3b). It can also be shown by the same derivation that the stress free boundary conditions are implicit in the energy related functional.

To solve (5) in terms of the unknown displacements, the following four steps have to be performed

- discretize solution domain into a finite number of elements
- find a stationary value for (5) with respect to u_x, u_y
- replace u_x, u_y by the approximations

$$u_x = [N(x,y)]\{u_x\}_e, \quad u_y = [N(x,y)]\{u_y\}_e$$

$$\frac{\partial u_x}{\partial x} = [\frac{\partial N(x,y)}{\partial x}]\{u_x\}_e, \quad \frac{\partial u_y}{\partial y} = [\frac{\partial N(x,y)}{\partial y}]\{u_y\}_e \text{ etc., where } [N(x,y)]$$

denotes the shape functions as a row vector with $\{u_x\}_e, \{u_y\}_e$ being the unknown displacements at the nodal points of each element. The resulting elemental matrix equation takes on the form

$$[K]\{u\}_e + [M]\ddot{\{u\}}_e = \{\bar{F}\}$$

or

$$\begin{bmatrix} [K_{xx}] & [K_{xy}] \\ [K_{yx}] & [K_{yy}] \end{bmatrix} \begin{Bmatrix} \{u_x\}_e \\ \{u_y\}_e \end{Bmatrix} + \begin{bmatrix} [M_x] & 0 \\ 0 & [M_y] \end{bmatrix} \begin{Bmatrix} \ddot{\{u_x\}}_e \\ \ddot{\{u_y\}}_e \end{Bmatrix} = \begin{Bmatrix} \{\bar{F}_x\} \\ \{\bar{F}_y\} \end{Bmatrix} \quad (6)$$

with the coefficients of the submatrices given by

$$K_{xx}(I,J) = \int [V_L^2 \frac{\partial N_I}{\partial x} \frac{\partial N_J}{\partial x} + V_s^2 \frac{\partial N_I}{\partial y} \frac{\partial N_J}{\partial y}] \rho dV$$

$$K_{xy}(I,J) = K_{yx}(J,I)$$

$$K_{xy}(I,J) = \int [(V_L^2 - 2V_s^2) \frac{\partial N_I}{\partial x} \frac{\partial N_J}{\partial y} + V_s^2 \frac{\partial N_I}{\partial y} \frac{\partial N_J}{\partial x}] \rho dV$$

$$K_{yy}(I,J) = \int [V_L^2 \frac{\partial N_I}{\partial y} \frac{\partial N_J}{\partial y} + V_s^2 \frac{\partial N_I}{\partial x} \frac{\partial N_J}{\partial x}] \rho dV$$

$$M_x(I) = M_y(I) = \int N_I N_J \rho dV$$

$\bar{F}_x(I), \bar{F}_y(I)$ are external driving forces. The numerical integration is carried out by employing a 7 point Gaussian quadrature formula.

- d) Assemble all the elemental matrices (6) into a global matrix which can be solved for $\{u_x\}$ and $\{u_y\}$. Before the assembly can be done however, the problem consists of integrating the second time derivative in (6). Possible integration schemes are termed as either explicit or implicit depending on whether a matrix inversion of $[K]$ is involved. The central difference integration (explicit) as well as the Houbolt, Wilson and Newmark integration (implicit) have been implemented. For the purposes of this paper only the Newmark integration is given

$$\begin{aligned} \left(\frac{1}{\alpha \Delta t^2} [M] + [K] \right) \{u\}_{t+\Delta t} = \{\bar{F}\}_{t+\Delta t} + \frac{1}{\alpha \Delta t} [M] \{u\}_t + \frac{1}{\alpha \Delta t} [M] \{\dot{u}\}_t + \\ + \left(\frac{1}{2\alpha} - 1 \right) [M] \{\ddot{u}\}_t \end{aligned}$$

This scheme can be made unconditionally stable depending on the selection of α and δ .

APPLICATIONS

In order to validate the finite element code, a bar subject to a step tension T_0 was modeled as shown in Figure 2. In Figure 3 the u_x displacement is plotted at three different locations A,B,C within the bar. The results are in excellent agreement with the one dimensional displacement predictions by Dewey et al. who also shows the analytical series solution.

A more crucial test results if one attempts to obtain the u_y displacements for a wide rectangular bar subject to a longitudinal step pressure loading. Jones and Ellis⁹ compared the theoretical predictions of the plane-stress theory with their experimental observations. Their experimental results for a 130 inch long and 1.5 inch wide bar with $V_s = 1.248 \times 10^5$ in/s and a Poisson ratio of $\sigma = 0.335$ also show good agreement with the finite element prediction shown in Figure 4. Typical solution times on a VAX 11/780 computer for two different mesh sizes are given in Table 1. These figures are somewhat misleading, however, since both mesh size and computer code are not yet optimized. In general, the computer time is a function of wave velocity, transducer frequency, sampling rate, distance of travel and mesh size. To illustrate this for a two dimensional case and show how a powerful computer like the CYBER 205 can significantly reduce the time requirement, consider the more sophisticated problem of pulse echo wave propagation as shown in Figure 5. Here a pulse created by a 1 MHz transducer propagates with a longitudinal velocity of $V_s = 5000$ m/s through a specimen of 12.5 cm thickness. The total travel time for twice the thickness is, therefore, 50 μ s. Based on an assumed sampling rate of 32 MHz it follows that 1600 time steps solution time are required. If a solution domain requiring a mesh size of 3000 nodes is assumed, it will take a VAX 11/780 computer about 4.5 minutes to solve the resulting matrix equation at each time step.

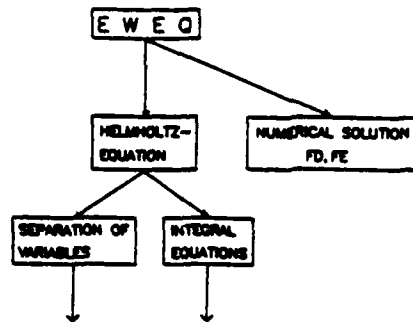


Fig. 1. Relationship between numerical (finite differences, finite elements) and analytical approaches

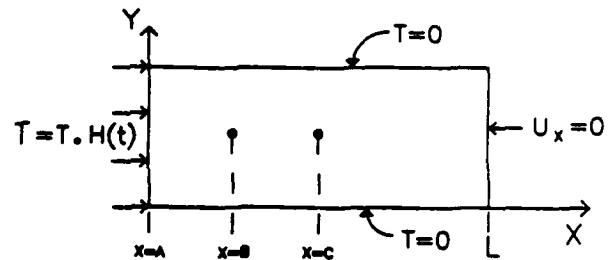


Fig. 2. Geometry and boundary conditions of rectangular bar

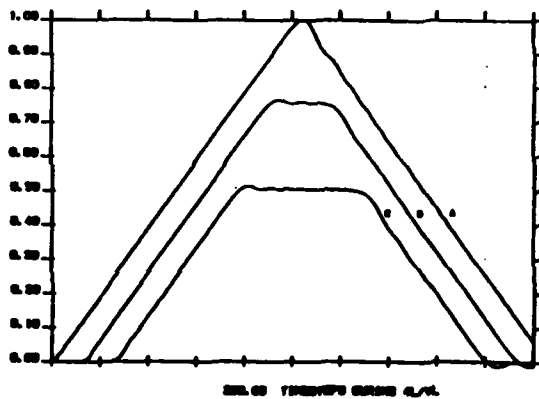


Fig. 3. Normalized u_x displacement at locations A, B, C

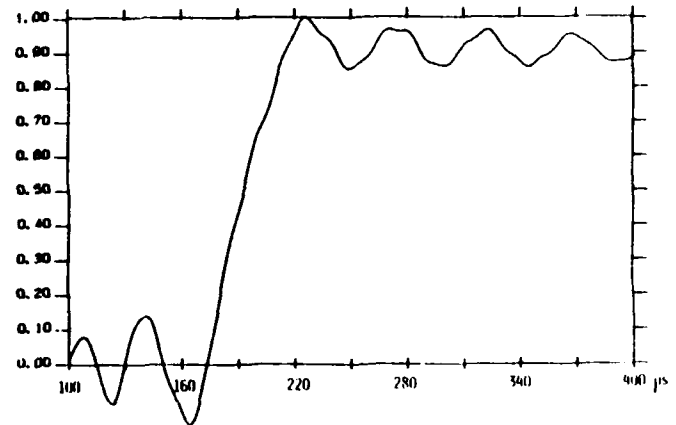


Fig. 4. Normalized u_y displacement at $x=37.5$ in.

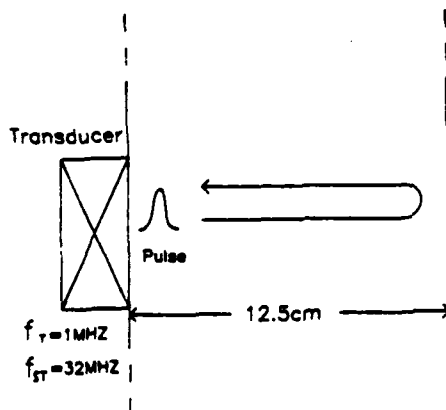


Fig. 5. Pulse echo time considerations

CP-requirements on VAX 11/780

| elements | nodes | CP-time(900 timesteps) |
|----------|-------|------------------------|
| 208 | 477 | 1h 51 min |
| 624 | 1325 | 8h 20 min |

Table 1. Solution time for transient bar analysis

Based on our experience with eddy current calculations, the CYBER 205 reduces the solution time to 0.0056 min. For a total of 1600 time steps this would amount to 120 hours on the VAX versus 9 minutes on the CYBER 205.

CONCLUSIONS

A considerable amount of work remains to be done before numerical code can be used as an engineering tool for the design and analysis of ultrasonic nondestructive tests. Early studies in this field show promise, however, and the increasing availability of supercomputers can provide the computational power needed to ultimately predict ultrasonic transducer responses from realistic defect geometries. Although the finite element formulation and applications described in this paper are 2-D in nature, only computational cost limits the extension to 3-D geometries.

ACKNOWLEDGMENTS

Support for this work has been provided by the Army Research Office and the Electric Power Research Institute. The authors have benefited from numerous discussions with Dr. Nathan Ida concerning the computational and programming aspects of finite element analysis. Douglas Moore's contributions to the development of the computer programs are greatly appreciated.

REFERENCES

1. W. Lord, Applications of Numerical Field Modeling to Electromagnetic Methods of Nondestructive Testing, IEEE Trans. Mag. 19:2437 (1983).
2. N. Ida, R. Palanisamy and W. Lord, Eddy Current Probe Design Using Finite Element Analysis, Mat. Eval. 41:1389 (1983).
3. R. Palanisamy and W. Lord, Sensitivity Analysis of a Variable Reluctance Probe for Steam Generator Tubing Inspection, IEEE Trans. Mag. 19:2219 (1983).
4. N. Ida and W. Lord, 3-D Finite Element Prediction of Magnetostatic Leakage Fields, IEEE Trans. Mag. 19:2260 (1983).
5. B. Allen and W. Lord, Finite Element Modeling of Pulsed Eddy Current Phenomena in "Review of Progress in Quantitative Nondestructive Evaluation," D. O. Thompson and D. E. Chimenti, eds., Plenum, New York (1983).
6. J. F. Gloudeman, The Anticipated Impact of Supercomputers on Finite Element Analysis, Proc. IEEE, 72:80 (1984).
7. L. J. Bond, Finite Difference Methods Applied to Ultrasonic Nondestructive Testing Problems, in "Review of Progress in Quantitative NDE," D. O. Thompson and D. E. Chimenti, eds., Plenum, New York (1980).
8. V. R. Dewey, B. F. Oliver and C. A. Picard, Finite Element Modeling of Ultrasonic Inspection of Weldments, in "Review of Progress in Quantitative NDE," D. O. Thompson and D. E. Chimenti, eds., Plenum, New York (1983).
9. O. E. Jones, A. T. Ellis, Longitudinal Strain Pulse Propagation in Wide Rectangular Bars, J. App. Mech. (1963).

END

FILMED

3-85

DTIC